

## Atomic Color Superfluid via Three-Body Loss

A. Kantian,<sup>1</sup> M. Dalmonte,<sup>1,2</sup> S. Diehl,<sup>1</sup> W. Hofstetter,<sup>3</sup> P. Zoller,<sup>1</sup> and A. J. Daley<sup>1</sup>

<sup>1</sup>*Institute for Theoretical Physics, University of Innsbruck, A-6020 Innsbruck, Austria,*

*and Institute for Quantum Optics and Quantum Information of the Austrian Academy of Sciences, A-6020 Innsbruck, Austria*

<sup>2</sup>*Dipartimento di Fisica dell'Università di Bologna and INFN, via Irnerio 46, 40127 Bologna, Italy*

<sup>3</sup>*Institute for Theoretical Physics, Johann Wolfgang Goethe-Universität, Frankfurt, Germany*

(Received 18 August 2009; revised manuscript received 13 November 2009; published 9 December 2009)

Large three-body loss rates in a three-component Fermi gas confined in an optical lattice can dynamically prevent atoms from tunneling so as to occupy a lattice site with three atoms. This effective constraint not only suppresses the occurrence of actual loss events, but stabilizes BCS-pairing phases by suppressing the formation of trions. We study the effect of the constraint on the many-body physics using bosonization and density matrix renormalization group techniques, and also investigate the full dissipative dynamics including loss for the example of <sup>6</sup>Li.

DOI: 10.1103/PhysRevLett.103.240401

PACS numbers: 03.75.Lm, 05.30.Jp, 42.50.-p, 67.85.Lm

Recent developments in the experimental control of degenerate Fermi gases with cold atoms [1] have paved the way for the study of three-component Fermi mixtures of different species or internal states [2]. For attractive two-body interactions, these systems offer a chance to observe competition between an atomic color superfluid phase, which has a BCS pairing of different components, and a phase of trions, formed of three atoms of different color [3–6]. In a broader context, color superfluids appear in different forms, e.g., in QCD [7]. A key feature of current atomic physics experiments, though (e.g., with lithium), is the large three-body loss rate observed in these mixtures [2]. Here we discuss how these high loss rates, which are normally undesirable, can give rise to an effective three-body hard-core constraint [8–11] when the gas is loaded into an optical lattice [12]. This constraint would stabilize the system, suppressing three-body occupation of lattice sites, and thus actual loss events. Moreover, trion formation will also be suppressed, enhancing pairing phases such as the atomic color superfluid.

Below we analyze this process quantitatively, focusing on a 1D system. This focus allows us (i) to compute the phase diagram in the presence of a constraint by combining Tomonaga Luttinger liquid (TLL) bosonization techniques with density matrix renormalization group (DMRG), and then (ii) to make quantitative predictions for the full non-equilibrium dynamics for realistic experimental parameters by combining time-dependent DMRG methods [13] with quantum trajectories techniques [8]. The consequences of the constraint are particularly striking in 1D because when all two-body interactions are attractive, the atomic color superfluid (ACS) phase is normally absent in the absence of the constraint (in fact BCS correlations decay exponentially). Instead, competition is observed between a charge-density wave (CDW) and a phase with symmetric (on-site) trions (ST) [4] [see Fig. 1(a)]. We show that the constraint prevents ST formation and produces an ACS phase with dominant, algebraically decaying BCS-pairing

correlations. This competes with a CDW and off-site trions (OT) [see Fig. 1(b)].

A three-component Fermi gas in the lowest band of an optical lattice is described by the Hamiltonian ( $\hbar = 1$ )

$$H_U = - \sum_{\langle i,j \rangle, \sigma} J_\sigma (c_{i,\sigma}^\dagger c_{j,\sigma} + \text{H.c.}) + \sum_{i,\sigma} U_\sigma m_{i,\sigma} m_{i,\sigma+1}, \quad (1)$$

where  $\langle i, j \rangle$  denotes a sum over neighboring sites,  $c_{i,\sigma}^\dagger, c_{i,\sigma}$  are fermionic operators with a species index  $\sigma = 1, 2, 3$ ,  $m_{i,\sigma} = c_{i,\sigma}^\dagger c_{i,\sigma}$ ,  $J_\sigma$  are the tunneling amplitudes, and  $U_\sigma$  are the on-site interaction energy shifts. In the following, we will consider balanced densities  $\bar{m}_\sigma = \bar{n}/3$  for total mean number density  $\bar{n}$ , and in typical realizations we will have equal tunneling amplitudes  $J_\sigma = J$ . This model is valid in the limit  $J_\sigma, U_\sigma \bar{n} \ll \omega$ , with  $\omega$  the energy separation between the lowest two Bloch bands.

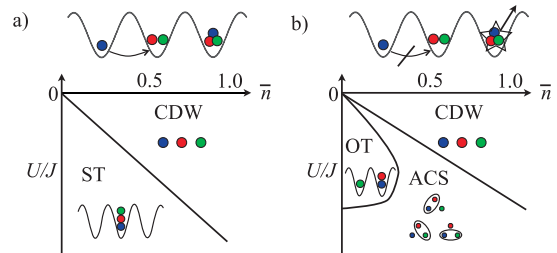


FIG. 1 (color online). Qualitative phase diagram for attractive interactions  $U < 0$  and equal populations  $\bar{n}/3$  of each component in a three-component 1D Fermi gas. These are shown in the SU(3) symmetric case (where all pairwise interactions between different components are of equal strength), (a) without and (b) with a three-body hard-core constraint arising from three-body loss. The unconstrained case is characterized by competition between symmetric (on-site) trions (ST) and a charge-density wave (CDW). The hard-core constraint suppresses trion formation, stabilizing BCS pairing in an atomic color superfluid (ACS), which competes with a CDW and off-site trions (OT).

Three-body recombination will result in decay into the continuum of unbound states, i.e., loss from the optical lattice. The decay dynamics can be described by a master equation in which loss occurs from a single site occupied by three atoms at a rate  $\gamma_3$  [8],

$$\dot{\rho}^{(N)} = -i[H_{\text{eff}}\rho^{(N)} - \rho^{(N)}H_{\text{eff}}^\dagger] + \gamma_3 \sum_i t_i \rho^{(N+3)} t_i^\dagger,$$

where  $\rho^{(N)}$  is the system density operator for a total number of  $N$  atoms,  $t_i = c_{i,1}c_{i,2}c_{i,3}$ , and the effective Hamiltonian is  $H_{\text{eff}} = H_U - i\gamma_3 t_i^\dagger t_i/2$ . If we begin with an initial state not involving three-body occupation, then via a mechanism analogous to the quantum Zeno effect, a large loss rate  $\gamma_3 \gg J$  will suppress coherent tunneling that would produce triply occupied sites. For large  $\gamma_3/J$ , loss occurs at an effective rate that decreases as  $J^2/\gamma_3$  in second-order perturbation theory. Then, on a time scale  $\sim \gamma_3/J^2$  where loss can be neglected, the system dynamics is described by the constrained Hamiltonian

$$H_C = \mathcal{P} H_U \mathcal{P}, \quad \mathcal{P} = \prod_j \mathcal{P}_j = \prod_j (1 - m_{j,1}m_{j,2}m_{j,3}),$$

where  $\mathcal{P}$  is a projector onto the subspace of states with at most two atoms per site.

*Overview.*—Below we first compute the ground state of  $H_C$  and determining the phase diagram in the presence of a perfect constraint. We treat both the SU(3) symmetric case where all interaction constants are equal (as could be realized, e.g., with nuclear spin states in alkaline earth atoms [14]), and the case where interactions are unequal (as is typical in lithium experiments at low magnetic fields [2]). We then return to the full picture of the nonequilibrium dynamics by computing time evolution under the master equation. This both allows us to test the assumption that loss probabilities are small on relevant experimental time scales, and to investigate time-dependent preparation of states. In particular, we investigate the production of an ACS state for the case of  ${}^6\text{Li}$  for typical experimental parameters.

*Determining the phase diagram.*—In 1D, the phase diagram is determined by identifying the dominant order in the system in different parameter regimes. To do this, we consider the behavior of correlation functions, and determine which is the strongest at long distances [15]. The orders shown in Fig. 1(b) are the following: CDW for which we compute the correlation function  $C(x) \propto \langle n_i n_{i+x} \rangle$  of the total density operator  $n_i = \sum_\alpha m_{i,\alpha}$ , ACS with BCS correlations  $P_\sigma(x) \propto \langle d_{i,\sigma}^\dagger d_{i,\sigma+1}^\dagger d_{i+x,\sigma} d_{i+x,\sigma+1} \rangle$  and OT with  $OT(x) \propto \langle \tilde{t}_{i,\sigma}^\dagger \tilde{t}_{i+x,\sigma} \rangle$  with  $\tilde{t}_{i,\sigma} = d_{i,\sigma} d_{i,\sigma+1} d_{i+1,\sigma+2}$ . Below we determine the behavior of these correlation functions via bosonization and DMRG methods, determining whether the decay is exponential or algebraic, and calculating decay exponents  $\mathcal{D}_{\text{CDW}}$ ,  $\mathcal{D}_{\text{ACS}}$ , and  $\mathcal{D}_{\text{OT}}$  in the case of the latter.

*Bosonization formalism for the constrained Hamiltonian.*—In order to apply the bosonization formal-

ism we identify an exact mapping of the constrained fermionic Hamiltonian  $H_C$  to an unconstrained fermionic Hamiltonian which automatically respects the constraint, at the expense of including higher order interactions. We introduce projected operators  $d_{i\sigma}^\dagger = (\prod_{j \neq i} \mathcal{P}_j) c_{i\sigma}^\dagger$ ,  $d_{i\sigma} = (\prod_{j \neq i} \mathcal{P}_j) c_{i\sigma}$ , entirely in terms of which we express the Hamiltonian. We verify (i) that the operators  $d_{i\sigma}$  obey fermionic commutations on the subspace where at most two atoms occupy any site, and that (ii) the Hamiltonian has vanishing matrix elements in the space with occupations greater than two and (iii) acts as zero on any state in this latter space. Thus, we arrive at a fermionic Hamiltonian with built-in constraint, which we analyze with standard bosonization techniques. Here we summarize the results, with the calculations presented in more detail in a forthcoming work [16]. We introduce three bosonic fields  $\phi_\sigma(x)$  related to the continuum version of  $(d_{i\sigma}^\dagger, d_{i\sigma})$ , from which we can construct a Hamiltonian by taking the linear combinations  $\phi_c = (\phi_1 + \phi_2 + \phi_3)/\sqrt{3}$ , which represents collective fluctuations of the total density, and  $\phi_{s1} = (\phi_1 - \phi_2)/\sqrt{2}$  and  $\phi_{s2} = (\phi_1 + \phi_2 - 2\phi_3)/\sqrt{6}$ , which represent the spin sectors. If we define TLL parameters  $K_\alpha$  and conjugate momentum fields  $\Pi_\alpha$  corresponding to each field  $\phi_\alpha$  ( $\alpha \in \{c, s1, s2\}$ ), we then obtain

$$H = \sum_{\alpha=c,s1,s2} \left\{ \frac{v}{2} \left[ K_\alpha \Pi_\alpha^2 + \frac{1}{K_\alpha} (\partial_x \phi_\alpha)^2 \right] \right\} - \frac{2g_{ss}}{a^2} \times \cos[\sqrt{2\pi}\phi_{s1}] \cos[\sqrt{6\pi}\phi_{s2}] - \frac{g_s}{a^2} \cos[\sqrt{8\pi}\phi_{s1}],$$

where  $v = 2aJ \sin[\pi\bar{n}/3]$  is the Fermi velocity,  $a$  is the lattice spacing. The coefficients  $g_{ss}$  and  $g_s$  exhibit non-trivial dependence on  $U/J$  and  $\bar{n}$ , as do  $K_\alpha$ .

The dependence of the decay exponents for different orders on  $K_\alpha$  can be extracted from the formalism, and by expanding  $K_\alpha$  in the weak interaction limit we obtain also the dependence on  $U/J$  and  $\bar{n}$ . We will present these formulas, which are not very compact, in a longer article [16]. The key results are summarized in the paragraph below, and are benchmarked against values extracted from numerical simulations in Table I.

*Phase diagram from bosonization.*—For comparison, the qualitative phase diagram for attractive interactions  $U_\sigma < 0$  in the absence of the hard-core constraint is depicted in Fig. 1(a). There are two phases, one with symmetric (on-site) trion (ST) order and the other with CDW order, which actually cross over into one another, the transition line marking where algebraic decay is equally strong. This was previously studied for equal attractive interactions using a combination of the TLL formalism and DMRG methods [4]. In a wide region near the SU(3) symmetric line  $U_\sigma = U < 0$ , CDW is dominant for higher densities and intermediate interactions. A particular feature of this case is that a gap appears in the entire spin sector, so that in contrast to a two-species Fermi gas, ACS correlations

TABLE I. Exponents for algebraic decay of correlations, computed for ground states in a system of 40 lattice sites with  $\bar{m}_\sigma = 0.2$  by fitting a power law to the periodic peaks of the correlations (see Fig. 2). Errors are given in parentheses, analytic values in the weak-coupling limit are given to the right of slashes. We find agreement with the qualitative predictions of analytic theory, i.e., for weak coupling we start out with the CDW-phase dominant, from where  $\mathcal{D}_{\text{CDW}}$  remains constant while  $\mathcal{D}_{\text{ACS}}$  and  $\mathcal{D}_{\text{OT}}$  decrease with increasing  $|U/J|$ . We further observe a transition to exponential decay for the off-site trions in the strong coupling limit.

$-U/J$	$\mathcal{D}_{\text{ACS}}$	$\mathcal{D}_{\text{CDW}}$	$\mathcal{D}_{\text{OT}}$
0.3	1.71(0.02)/2.04	1.39(0.02)/1.95	3.3(0.3)/3.00
0.6	1.66(0.02)/2.03	1.40(0.03)/1.96	3.3(0.3)/3.00
1	1.60(0.02)	1.40(0.03)	3.1(0.4)
2	1.4(0.2)	1.4(0.1)	3.0(0.4)
5, 8, 10	1.4(0.4)	1.4(0.3)	exp

decay exponentially (as do spin-density wave correlations).

In the presence of the constraint this picture changes substantially [see Fig. 1(b) with small  $|U/J|$ ]. The ST phase is suppressed by the constraint, and for most regions of the diagram the spin sector is gapless, so that all correlations decay algebraically. We observe competition between an OT, a CDW, and an ACS phase, which for equal interactions involves simultaneous pairing of all three pairs of components. The only exception to this is at low densities  $\bar{n} < 0.2$  and intermediate interactions, where bosonization results predict a second-order transition below which ACS correlations again decay exponentially and OT correlations dominate over CDW correlations. At higher densities, there is a crossover from the ACS to the CDW phase. In the case of unequal interactions, the charge sector and two spin sectors are coupled [16]. For sufficiently strong imbalance in  $U_\alpha$  a gap in the spin sector may open, so that only BCS pairing for the channel with the largest  $|U_\alpha|$  survives.

*Ground state of  $H_C$  from DMRG (equal interactions).*—To underpin these results quantitatively and go beyond weak coupling, we present calculations based on DMRG methods [13]. In Fig. 2(a), we see again the striking comparison between the ACS correlations in the ground states for  $H_U$  and  $H_C$ , which exhibit exponential decay without the hard-core constraint, and algebraic decay in the presence of the constraint. In Figs. 2(b) and 2(c) we show a comparison of the correlations corresponding to the ACS [ $P_\sigma(x)$ ], CDW [ $C_\sigma(x)$ ] and OT [ $OT(x)$ ], in the ground state of the model with a three-body hard-core constraint ( $H_C$ ). These are presented for symmetric but varying interactions from weak to strong coupling,  $U/J \in [-10, -0.3]$ . For increasing interactions, the values of  $P_\sigma(x)$  become larger with respect to  $C_\sigma(x)$ , so that the ACS appears to dominate for stronger interactions. While off-site trions still show algebraic decay for  $U/J \geq -2$ , they are subdominant to the ACS and CDW, and they decay exponentially for

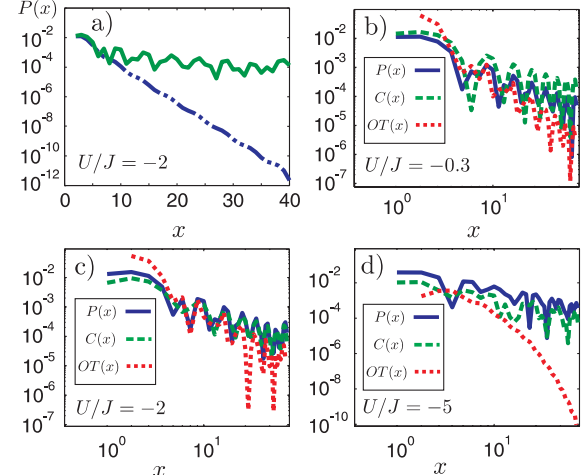


FIG. 2 (color online). (a) ACS correlations  $P_\sigma(x)$  with (solid line) and without (dash-dotted line) the three-body constraint as a function of distance  $x$  on a 40 site lattice. (b)–(d)  $P_\sigma(x)$  with CDW-correlations  $C(x)$  and off-site trion correlations  $OT(x)$  for different values of  $U$ , at a density  $\bar{m}_1 = \bar{m}_2 = \bar{m}_3 = 0.2$ , with the constraint. In qualitative agreement with bosonization, we observe that for weak coupling (b) CDW clearly dominates. As the coupling is increased (b)–(d), ACS appears to dominate. For the values shown here, ACS dominates off-site trions, with  $OT(x)$  decaying exponentially for strong coupling.

$U/J \leq -5$  [Figs. 2(b)–2(d)]. This is a strong deviation from the weak-coupling bosonization results, and could indicate an instability (e.g., towards phase separation), or the appearance of a gap in the dual field of the charge sector. However, with system sizes of 40 lattice sites, we have not observed any evidence of phase separation.

Extracting the exponents of the algebraic decay of the correlation functions further confirms this picture, as shown in Table I. The constrained model sees an enhancement of ACS correlations with decreasing  $U$ , while CDW correlations generally decay faster as  $U$  is lowered. In the weak coupling regime we also generally observe good agreement with the perturbative values of the exponents from TLL theory. In the strong coupling regime ( $U/J \leq -5$ ) for the constrained case, the exponents  $\mathcal{D}_{\text{ACS}}$  and  $\mathcal{D}_{\text{CDW}}$  saturate, with  $\mathcal{D}_{\text{ACS}}$  taking a value compatible with the TLL prediction.

*Ground state of  $H_C$  from DMRG (unequal interactions).*—In the case of asymmetric interactions we also observe an ACS pairing, but with only the two components paired that exhibit the strongest interactions. As an example, we consider the case of  ${}^6\text{Li}$ , where in Fig. 3(a) we plot the Hamiltonian parameters as a function of magnetic field strength near 500–700 G for a fixed lattice depth. From the pairing correlations shown in Fig. 3(b), we see that at 500 G, the only algebraically decaying correlations are those corresponding to components 1 and 3, which have the strongest interparticle interaction.

*Time-dependent preparation of an ACS phase with  ${}^6\text{Li}$ .*—Considering this example, we now return to the

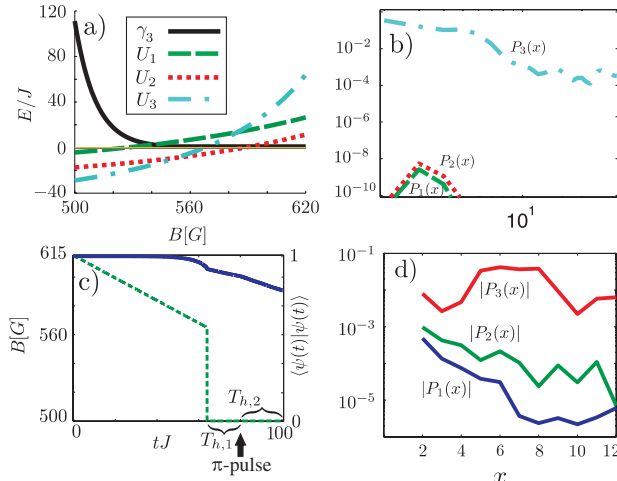


FIG. 3 (color online). (a) Hubbard parameters  $U_1$ ,  $U_2$ ,  $U_3$  and three-body loss rate  $\gamma_3$  for  ${}^6\text{Li}$  as function of external magnetic field  $B$ , for a lattice depth of  $V_{ax} = 5 E_R$  in axial direction, and  $V_{rad} = 20 E_R$  in radial direction. (b) ACS correlations for the ground state of  $H_C$  at  $B = 500$  G, computed for a system of 30 lattice sites,  $\bar{m}_\sigma = 2/15$ ,  $\sigma = 1, 2, 3$ . The dash-dotted line shows  $P_3(x)$ , dashed line  $P_1(x)$ , dotted line denotes  $P_2(x)$ . As  $U_3 < U_2 \ll U_1$ , we see 1–3 pairing dominate, with all other pairing exponentially suppressed. (c) Left scale, dashed line: Magnetic field  $B(t)$  for the ramp. Right scale, solid line: Probability of no three-body loss having occurred at time  $t$ . (d) ACS correlations after the time-dependent ramp of the magnetic field shown in (c), beginning from the ground state at 615 G, with  $\bar{m}_\sigma = 0.167$ , on 12 sites.

full time-dependent dynamics including three-body loss, in order to demonstrate a method to produce these ACS states in  ${}^6\text{Li}$ . We simulate the many-body master equation on 12–24 lattice sites by combining time-dependent DMRG methods with quantum trajectories techniques, as described in [8]. We assume that the lattice is initially loaded at a magnetic field of 615 G, where the repulsive interactions [see Fig. 3(a)] will stabilize the system in the presence of loss. We then consider a time-dependent ramp of the magnetic field to 500 G. The characteristics of the ramp we choose [shown in Fig. 3(c)] are the following: (i) it is adiabatic until 565 G, where the components 2 and 3 become paired, (ii) it is fast from 565–500 G, where on-site trions become energetically favored ( $\sum_\alpha U_\alpha < U_2$ ) and where for fields larger than 520 G,  $\gamma_3$  is too small to prevent triple occupation [see Fig. 3(a)], and (iii) after a hold time  $T_{h,1} = 16J^{-1}$  we add a swap between species 1 and 2 via a fast laser pulse at the end of the ramp, after which there is a second hold time  $T_{h,2} = 20J^{-1}$ . The ACS correlations in the final state after the swap [Fig. 3(d)] then exhibit dominant pairing between species 1 and 3, as would be expected in the ground state for the parameters of  ${}^6\text{Li}$  at  $B = 500$  G with the constraint. The other pairing channels are clearly subdominant, and trion formation is also strongly suppressed during the ramp ( $\max[T(x)] \approx$

$\mathcal{O}(10^{-8})$ ). The probability that no decay event occurs during the ramp shown here for 12 lattice sites is 79%.

In higher dimensions, we expect that actual losses will be suppressed on a lattice by the effect discussed here, and that the ACS phase [3] will also be stabilized due to suppressed trion formation.

We thank S. Jochim, M. Fleischhauer, P. Julienne, M. Baranov, and E. Ercolessi for discussions. Work in Innsbruck was supported by the Austrian Science Foundation (FWF) through SFB F40 FOCUS and project I118\_N16 (EuroQUAM\_DQS), the DARPA OLE program and by the Austrian Ministry of Science BMWF via the UniInfrastrukturprogramm of the Forschungsplattform Scientific Computing and Centre for Quantum Physics, and in Frankfurt by the DFG through SFB/TR 49.

- [1] R. Jördens *et al.*, Nature (London) **455**, 204 (2008); C. H. Schunck, Y. Shin, A. Schirotzek, and W. Ketterle, *ibid.* **454**, 739 (2008); J. T. Stewart, J. P. Gaebler, and D. S. Jin, *ibid.*, **454**, 744 (2008); U. Schneider *et al.*, Science **322**, 1520 (2008); E. Wille *et al.*, Phys. Rev. Lett. **100**, 053201 (2008); A. Schirotzek, C.-H. Wu, A. Sommer, and M. W. Zwierlein, *ibid.* **102**, 230402 (2009).
- [2] T. B. Ottenstein *et al.*, Phys. Rev. Lett. **101**, 203202 (2008); J. H. Huckans *et al.*, *ibid.* **102**, 165302 (2009).
- [3] A. Rapp, G. Zarand, C. Honerkamp, and W. Hofstetter, Phys. Rev. Lett. **98**, 160405 (2007); A. Rapp, W. Hofstetter, and G. Zarand, Phys. Rev. B **77**, 144520 (2008).
- [4] S. Capponi *et al.*, Phys. Rev. A **77**, 013624 (2008); P. Azaria, S. Capponi, and P. Lecheminant, *ibid.* **80**, 041604(R) (2009).
- [5] A. G. K. Modawi and A. J. Leggett, J. Low Temp. Phys. **109**, 625 (1997).
- [6] R. W. Cherng, G. Refael, and E. Demler, Phys. Rev. Lett. **99**, 130406 (2007).
- [7] K. Rajagopal and Frank Wilczek, in *At the Frontier of Particle Physics, Handbook of QCD*, edited by M. Shifman (World Scientific, Singapore, 2001), p. 2061.
- [8] A. J. Daley *et al.*, Phys. Rev. Lett. **102**, 040402 (2009).
- [9] M. Roncaglia, M. Rizzi, and J. I. Cirac, arXiv:0905.1247.
- [10] N. Syassen *et al.*, Science **320**, 1329 (2008).
- [11] J. J. Garcia-Ripoll *et al.*, New J. Phys. **11**, 013053 (2009).
- [12] I. Bloch, J. Dalibard, and W. Zwerger, Rev. Mod. Phys. **80**, 885 (2008).
- [13] G. Vidal, Phys. Rev. Lett. **93**, 040502 (2004); F. Verstraete, V. Murg, and J. I. Cirac, Adv. Phys. **57**, 143 (2008); A. J. Daley *et al.*, J. Stat. Mech. (2004) P04005; S. R. White and A. E. Feiguin, Phys. Rev. Lett. **93**, 076401 (2004); F. Verstraete, J. J. Garcia-Ripoll, and J. I. Cirac, *ibid.* **93**, 207204 (2004).
- [14] A. V. Gorshkov *et al.*, arXiv:0905.2610.
- [15] A. O. Gogolin, A. A. Nersesyan, and A. M. Tsvelik, *Bosonization and Strongly Correlated Systems* (Cambridge University press, Cambridge, 1998); T. Giamarchi, *Quantum Physics in One Dimension* (Oxford University press, Oxford, 2003).
- [16] M. Dalmonte *et al.* (to be published).